Int J Legal Med (2010) 124:397–404
DOI 10.1007/s00414-010-0465-1

ORIGINAL ARTICLE

The cannabinoid receptor type 2 is time-dependently expressed during skeletal muscle wound healing in rats

Tian-Shui Yu · Zi-Hui Cheng · Li-Qiang Li · Rui Zhao · Yan-Yan Fan · Yu Du · Wen-Xiang Ma · Da-Wei Guan

Received: 3 February 2010 / Accepted: 29 April 2010 / Published online: 11 June 2010

Abstract The expression of the cannabinoid receptor type 2 (CB2R) was investigated by immunohistochemistry, Western blotting, and RT-PCR during wound healing of contused skeletal muscle in rats with attempt of its applicability to skeletal muscle wound age estimation. Furthermore, Macrophage Marker (MAC387) was utilized to identify macrophages recruited into injured skeletal muscle tissue. Co-localization of CB2R with Macrophage Marker was detected by confocal laser scanning microscopy. A total of 50 Sprague–Dawley male rats were divided into control and contusion groups (3 h, 6 h, 12 h, 1 day, 3 days, 5 days, 7 days, 10 days, and 14 days post-injury). In the uninjured controls, immunoreactivity of CB2R was detected in the sarcolemma and sarcoplasm of normal myofibers. In the contusion groups, a few polymorphonulcear cells, a large number of macrophages, and spindle-shaped fibroblastic cells showed a positive staining for CB2R in wounded zones. By Western blotting analysis, the average of CB2R to GAPDH ratios in 5–7 days post-injury groups was highest, and all the samples had ratios of >2.60. In the other groups, no samples showed ratios of >2.60 and the CB2R to GAPDH ratios ranged from 1.19 to 2.59. The expression tendency was also confirmed by RT-PCR. From the viewpoint of forensic pathology, these observations suggested that the ratio markedly exceeding 2.60 strongly indicated a wound age of 5–7 days. In conclusion, dynamic distribution and expression of CB2R suggest that CB2R be involved in modulating macrophages in response to inflammatory event in rat skeletal muscle wound healing and CB2R be available as a marker for wound age determination.

Keywords Forensic pathology · Wound age determination · Skeletal muscle contusion · CB2R · Macrophage

T.-S. Yu · Z.-H. Cheng · L.-Q. Li · R. Zhao · Y.-Y. Fan · Y. Du · W.-X. Ma · D.-W. Guan (✉)
Department of Forensic Pathology,
China Medical University School of Forensic Medicine,
No.92, Beier Road, Heping District,
Shengyang, Liaoning Province 110001,
People's Republic of China
e-mail: dwguan@mail.cmu.edu.cn

Introduction

The endogenous cannabinoid system consists of the cannabinoid receptor type 1 and 2 (CB1R and CB2R), the endogenous ligands (endocannabinoids), and enzymes that synthesize and degrade endocannabinoids. CB2R is first identified in macrophages in the marginal zone of spleen [1]. It is currently accepted that CB2R is found mainly on the surface of immune cells including neutrophils, monocytes, natural killer cells, eosinophils, mast cells, dendritic cells, and subtypes of B and T cells in vitro [2–9]. Recently, CB2R is also detected on macrophages in the colonic lamina propria [10].

When skeletal muscle is damaged, the tissue repair process starts immediately and is a complicated but well-organized biological phenomenon concomitant with polymorphonulcear cells (PMNs) and round-shaped mononuclear cells (MNCs) infiltration-macrophages, spindle-shaped fibroblastic cells (FBCs) proliferation, composed of three different phases, destruction, repair, and remodeling. Although the physiological roles of CB2R, mainly expressed in kinds of inflammatory cells, have not yet been elucidated during skeletal muscle wound healing, recent researches have shown that CB2R is closely involved in several types of tissue injury repair. CB2R activation reduces the PMN-dependent myocardial I/R damage with a reduction of oxidative stress and neutrophil

infiltration in the infarcted myocardium [11]. Activating CB2R with its selective agonist JWH-133 protects against hepatic I/R damage by decreasing histological damage and neutrophil infiltration 24 h following ischemia [12]. Furthermore, macrophages, deriving from resident microglia and/or invading monocytes, appear CB2R positive on the lesioned side of the brain at day 3 after hypoxic–ischemia and middle cerebral artery occlusion [13]. Besides, the effect of activating CB2R with JWH-133 significantly decreases hepatic fibrosis as compared with cirrhotic rats treated with vehicle [14]. In addition, it has been universally acknowledged that CB2R regulates mRNA expression of key genes involved in nutrient oxidation and energy metabolism in both human and rodent skeletal muscle [15]. Based on all of studies mentioned above, tenable hypotheses are that CB2R may participate in inflammatory and fibrous repair process after skeletal muscle contusion in rats.

In the present study, we have immunohistochemically investigated occurrence and distribution of CB2R during skeletal muscle wound healing, with special emphasis on the immunolocalization of CB2R in macrophage. Moreover, time-dependent expression of CB2R was examined by Western blotting and RT-PCR using an established model to discuss its practical suitability as a parameter for wound age determination.

Materials and methods

Animal model of skeletal muscle contusion

We established a standardized animal model of skeletal muscle contusion in rats, which was controllable and reproducible well using a self-designed mechanical weight-drop device. Since instant impact velocity (V) and elastic deformation (DF) at the time of impact are key parameters for impact intensity [16], V and DF were monitored and recorded during the present experimentation, which might make severity of contusion identical as far as possible. Briefly, a total of 50 healthy, adult Sprague–Dawley male rats, weighing between 280 and 320 g, were divided into contusion group and control group. Of 50 rats, 45 were anesthetized by intraperitoneal injection with 2% sodium pentobarbital (30 mg/kg). Subsequently, the rats were placed on experimental table in a prone position, and a single impact at velocity of 3 m/s was delivered to the site of the right posterior limb 2.5 cm away from calcaneus with 7.5 mm for DF. The size of impact interface of the counterpoise (weighing 500 g) was 1.127 cm^2. The energy transmitted to the right posterior limb was calculated to be 2.25 J as calculated by the equation: $E=1/2mv^2$. After wounding, each rat was individually housed in a cage and fed with commercial rat chow and tap water ad libitum. All animals were kept under a 12 h light–dark cycle with specific pathogen-free conditions. After the animals were killed by intraperitoneal injection of an overdose of sodium pentobarbital (350 mg/kg) at 3 h, 6 h, 12 h, 1 day, 3 days, 5 days, 7 days, 10 days, and 14 days after impact (five rats each time interval), muscle specimen was taken from wound site and equally divided into two blocks. One block was used for immunohistochemical procedure, and another was used for Western blotting and RT-PCR, respectively. The remaining five rats were used as control, and samples were dissected from the same site after anesthetization with over dose of pentobarbital. No bone fracture was detected at dissection.

Experiments were conformed to the "Principles of Laboratory Animal Care" (National Institutes of Health published no 85-23, revised 1985) that sought to minimize both the number of animals used and any suffering that they might experience and were performed according to the Guidelines for the Care and Use of Laboratory Animals of China Medical University.

Tissue preparation and immunohistochemical staining

The skeletal muscle specimens were immediately fixed in 4% paraformaldehyde in phosphate-buffered saline (pH 7.4) and embedded in paraffin. Five-micrometer-thick sections were prepared. Immunostaining was performed using the streptavidin–peroxidase method. Briefly, tissue sections were mounted on the APES-coated glass slides. The sections were deparaffinized in xylene, rehydrated with a series of graded alcohol, and then heated in 0.01 mol/L sodium citrate buffer (pH 6.0) with a medical microwave oven for antigen retrieve. Subsequently, hydrogen peroxide (3%) was applied for quenching endogenous peroxidase activity. The sections were blocked with 10% non-immune goat serum to reduce non-specific binding. Then tissue sections were incubated with rabbit anti-CB2 polyclonal antibody (dilution 1:400; sc-25494, Santa Cruz Biotechnology, CA, USA) overnight at 4°C, followed by incubation with Histostain-*Plus* Kit according to the manufacturer's instructions (Zymed Laboratories, South San Francisco, CA, USA). The sections were routinely counterstained with hematoxylin. As immunohistochemical controls for immunostaining procedures, some sections were incubated with normal rabbit IgG or PBS in place of the primary antibody. Hematoxylin–eosin (H-E) staining was conventionally conducted.

Double indirect immunofluorescence and multichannel confocal microscopy analysis

Briefly, deparaffinized sections were blocked with 5% BSA and incubated with rabbit anti-CB2R polyclonal antibody

(dilution 1:50; sc-25494, Santa Cruz Biotechnology) at room temperature for 2 h. Thereafter, the sections were further incubated with biotinylated donkey anti-rabbit IgG (dilution 1:200; ab6801, Abcam, Cambridge, UK) and streptavidin, Alexa Fluor® 555 conjugate (dilution 1:200; S-21381, Invitrogen, CA, USA). Then, tissue sections were incubated with mouse anti-Macrophage Marker (MAC387) monoclonal antibody (dilution 1:50; sc-66204, Santa Cruz Biotechnology) overnight at 4°C. After incubation with Alexa Fluor® 488 donkey anti-mouse IgG (dilution 1:200; A21202, Invitrogen) at room temperature for 2 h, the nuclei were routinely counterstained with Hoechst 33258. Normal rabbit or mouse IgG was used instead of primary antibodies as negative control. The sections were observed by confocal microscopy with parameters as follows.

A laser confocal scanning microscope system (FV1000S, Olympus, Japan), mounted on an inverted optical microscope (IX81, Olympus, Japan), was used. The observation and image acquisition, using a ×60 oil immersion objective lens (numerical aperture 1.4), were performed by 405-nm excitation/460-nm emission for Hoechst 33258, 488-nm excitation/519-nm emission for Alexa Fluor® 488 and 559-nm excitation/565-nm emission for Alexa Fluor® 555. In order to test for co-localization, a single section at the same focus plane was scanned at 0.62 μm thickness in *z*-axle, and the three channels were merged into a 12-bit RGB tif-file by using FV1000 Viewer (Ver.1.6b) software. After recording by confocal laser scanning microscopy, no alternations of image files were performed by additional image processing.

Protein preparation and immunoblotting assay

The skeletal muscle samples were diced into very small pieces using a clean razor blade and homogenized with a sonicator in RIPA buffer (sc-24948, Santa Cruz Biotechnology) containing protease inhibitors at 4°C. Homogenates were centrifuged at 12,000×*g* for 30 min at 4°C three times, and the resulting supernatants were collected. The protein concentrations were determined by Lowry method. Aliquots of the supernatants were diluted in an equal volume of 5× electrophoresis sample buffer and boiled for 5 min. Protein lysates (40 μg) were separated on a 12% sodium dodecyl sulfate–polyacrylamide electrophoresis gel and transferred onto polyvinylidene fluoride membranes (Millipore, Billerica, MA, USA). After being blocked with 5% non-fat dry milk in Tris-buffered saline-Tween#20 at room temperature for 2 h, the membranes were incubated with rabbit anti-CB2R polyclonal antibody (dilution 1:600; sc-25494, Santa Cruz Biotechnology) at 4°C overnight and horseradish peroxidase conjugated goat anti-rabbit IgG (sc-2004, Santa Cruz Biotechnology) at 1:8,000 dilution at room temperature for 2 h. The blotting was visualized with Western blotting luminol reagent (sc-2048, Santa Cruz Biotechnology) by Electrophoresis Gel Imaging Analysis System (MF-ChemiBIS 3.2, DNR Bio-Imaging Systems, ISR). Subsequently, densitometric analyses of the bands were semi-quantitatively conducted using Scion Image Software (Scion Corporation, MD, USA). The relative protein levels were calculated by comparison with the amount of GAPDH (#G13-61M, signalchem, Canada) as a loading control.

Total RNA extraction and reverse transcription PCR

Total RNA was extracted from the skeletal muscle specimens with RNAiso Plus (9108, Takara Biotechnology, Shiga, Japan) according to the manufacturer's instructions. The RNA pellet was air-dried for 10 min and resuspended in 15 μl diethylpyrocarbonate-treated dH_2O. Using 1 μl RNA samples, cDNA synthesis was performed in a 9-μl reaction mixture containing 2 μl $MgCl_2$, 1 μl 10× RT buffer, 3.75 μl RNase-free dH_2O, 1 μl dNTP mixture, 0.25 μl RNase inhibitor, 0.5 μl Avian Myeloblastosis Virus Reverse Transcriptase (AMV-RT), and 0.5 μl Random 9 mers provided by TaKaRa RNA PCR Kit (AMV) Ver.3.0 (RR019, Takara Biotechnology, Shiga, Japan). The reaction mixture was incubated at 30°C for 10 min twice, 42°C for 30 min, 99°C for 1 min, followed by 5 min at 5°C. The resulting cDNA was used for PCR with the sequence-specific primer pairs for CB2R and GAPDH. PCR amplification was performed in a 60-μl reaction mixture which contained 12.5 μl 5× PCR buffer, 36 μl sterile H_2O, 0.5 μl *TaKaRa Ex Taq*, 0.5 μl forward primer, 0.5 μl reverse primer, and 10 μl cDNA. After initial denaturation at 94°C for 2 min, amplification consisting of denaturation at 94°C for 40 s, annealing at 60°C for 40 s, and extension at 72°C for 1 min was performed for 35 cycles for GAPDH and 36 cycles for CB2R. The amplified PCR products were identified using electrophoresis of 6 μl aliquots on a 2% agarose gel and were stained with Genefinder (204001, Bio-V, Xiamen, China). To exclude any potential genomic DNA contamination, each PCR was also performed without the RT step. No DNA amplification product was detected. All PCRs were repeated at least three times for each cDNA. For normalization of the amount of different cDNAs, GAPDH was used as an internal standard. The specific primers of CB2R and GAPDH were shown in Table 1.

The products were visualized with Electrophoresis Gel Imaging Analysis System (ChemiImager 5500, Alpha Innotech, USA). Labworks Image Acquisition and Analysis Software (UVP Inc., Upland, CA, USA) were employed for the semi-quantitative digital image analysis of the band of the PCR product. The ratio of CB2R to GAPDH band intensity was calculated to normalize the determined value.

Table 1 Primer sequences used for reverse transcription polymerase chain reaction

Gene	Species	Primer	Position	Product size (bp)
CB2	Rodent	Forward: 5′-TTC CCC CTG ATC CCC AAC GAC TA-3′ Reverse: 5′-CTC TCC ACT CCG CAG GGC ATA AAT-3′	547–569 892–915	369
GAPDH	Rodent	Forward: 5′-CAG CAA TGC ATC CTG CAC-3′ Reverse: 5′-GAG TTG CTG TTG AAG TCA CAG G-3′	506–523 900–921	416

Numbers (NM_) of the genes are NCBI accession numbers obtained from the NIH Database for rodent (R): CB2, (R) NM_020543; GAPDH, (R) NM_X02231

CB2 cannabinoid receptor type 2, *GAPDH* glyceraldehyde-3-phosphate dehydrogenase

Statistical analysis

Data were expressed as means±standard deviation and analyzed using SPSS for Windows 11.0. The one-way ANOVA was used for data analysis between two groups. Difference associated with $P<0.05$ was considered statistically significant.

Results

Histological examination and immunostaining with CB2R and Macrophage Marker

In sections stained with hematoxylin and eosin, hemorrhage, edema, and degeneration were present in contused skeletal muscle, and a few PMNs appeared at wound zones at 3 and 6 h post-wounding. A large number of PMNs and MNCs accumulated in the wounds and necrotized skeletal muscle fibers were phagocytosed gradually at 12 h and 1 day post-injury. MNCs remained abundant from 3 to 7 days after wounding. From 3 days post-injury onward, FBCs were present in the wound zones, and multinucleated myotubes augmented remarkably at 5–7 days (Fig. 1a–d).

In the uninjured skeletal muscle specimens, weakly positive immunoreactivity for CB2R was detected in the sarcolemma, sarcoplasm (Fig. 2a), and vascular smooth muscle cells. In the injured skeletal muscle samples, various staining patterns were present. No false positive staining was detected in the sections used as immunohistochemical controls. CB2R was positive in a few of PMNs. Afterwards, CB2R positive staining was observed in round-shaped MNCs and spindle-shaped FBCs (Fig. 2b, d) in contusion zones. Immunostaining for CB2R were also detected in the contused skeletal muscle fibers near wound site and regenerated multinucleated myotubes (Fig. 2c) in areas of

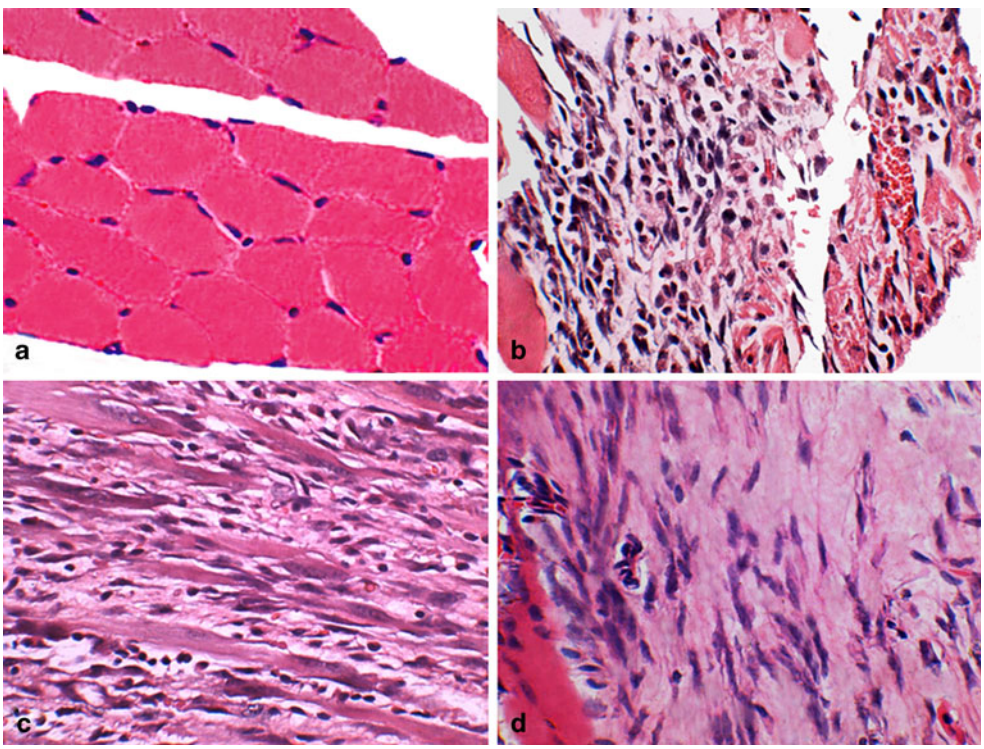

Fig. 1 Histological analysis in rat skeletal muscle contusion. **a** The morphology of normal skeletal muscle is confirmed with the H-E stain in the control. **b** FBCs are present in the injured tissue, and damaged muscle fibers are mostly phagocytosed at 3 days post-injury. **c**, **d** The wound healing becomes more prominent with extension of posttraumatic interval. A large number of spindle-shaped FBCs, concomitant with regenerated multinucleated myotubes, accumulate in the area of contusion at 5 and 14 days post-wounding (original magnification, ×400)

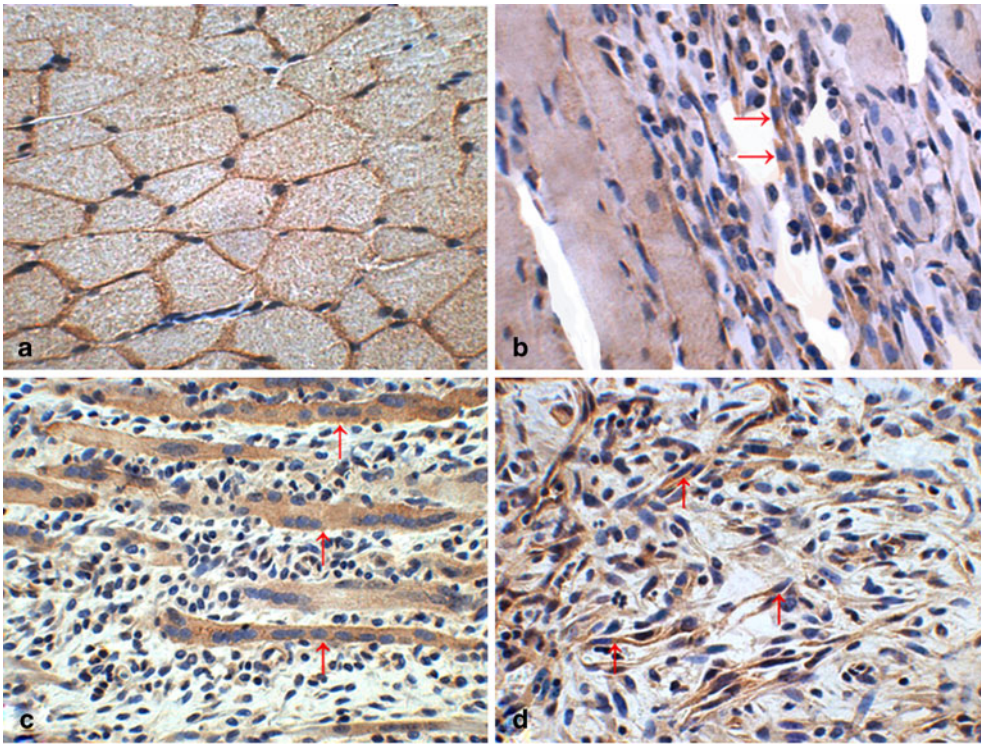

Fig. 2 Immunohistochemical staining of CB2R in rat skeletal muscle contusion. **a** CB2R immunoreactivity is found in the sarcolemma and sarcoplasm of normal myofibers in the uninjured control. **b** CB2R-positive spindle-shaped FBCs (*arrows*) are detected in the area of contusion at 3 days post-injury. **c**, **d** Multinucleated myotubes (*arrows*) and spindle-shaped FBCs (*arrows*) are positively immunostained with antibody against CB2R in the area of contusion at 5 and 14 days after injury (original magnification, ×400)

skeletal muscle wound healing. Moreover, vascular smooth muscle cells of new vessels showed positive staining for CB2R.

For identification of MNCs, co-localization of CB2R and Macrophage Marker were conducted by double indirect immunofluorescent method. In control group, a few of $CB2R^{+}$/Macrophage $Marker^{+}$ positive cells were observed in the perimysium and epimysium of normal skeletal muscle, indicating that resident tissue macrophages were CB2R positive. In 1 day post-injury group, a great quantity of MNCs infiltrated into injured site showed wide $CB2R^{+}$/Macrophage $Marker^{+}$ positive (Fig. 3). With extension of

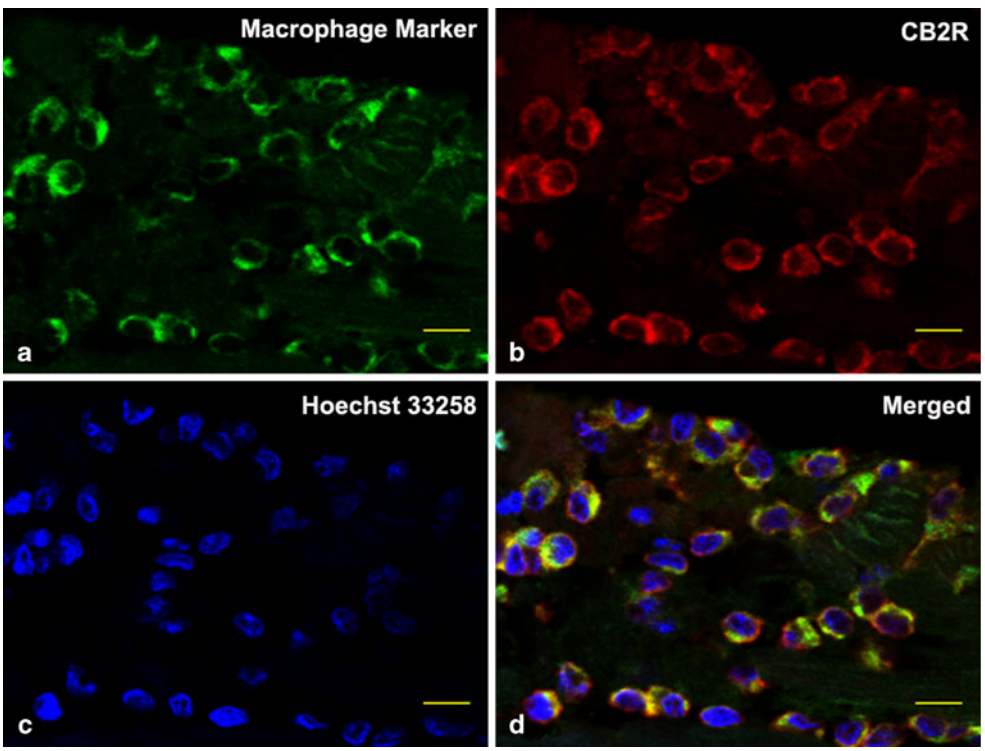

Fig. 3 Double immunofluorescence analysis was performed to determine CB2R-expressing macrophages at 1 day post-injury. The samples were immunostained with anti-Macrophage Marker (**a**, *green*) and anti-CB2R (**b**, *red*). Image (**d**, *yellow*) of Macrophage Marker and CB2R co-localization was digitally merged within injured area. Nuclei were counterstained with Hoechst 33258 (**c**, *blue*). Representative results from at least three individual experiments are shown here. Scale bars=10 μm

posttraumatic interval, the less double-positive MNCs were detectable at the wound sites.

Western blotting and RT-PCR

The blots against CB2R antibody were showed under the experimental conditions and CB2R protein expression was increased nearly twofold as early as 1 day and remained elevated until 14 days after skeletal muscle contusion (Fig. 4a). Peak values in the average ratios of CB2R to GAPDH were 2.70±0.08 and 2.69±0.07 at 5 and 7 days post-injury, respectively. In the other groups, the CB2R to GAPDH ratios were shown in Table 2. Significant differences in the relative expression levels of CB2R protein were found between control group and each posttraumatic interval. There were significant differences in the relative intensity of CB2R to GAPDH between 3 h, 6 h, 12 h, 5 days, 10 days, and, 14 days injury groups and their preceding groups as shown in Fig. 4b.

CB2R mRNA could be detected in all skeletal muscle samples, and mRNA expression of CB2R in contusion groups was significantly augmented as compared with control groups (Fig. 5a). Similar to Western blotting results, the mean ratios of CB2R to GAPDH reached its climaxes at 5 and 7 days after injury. There was significant difference in the relative intensity of CB2R to GAPDH between control group and each posttraumatic interval, between 3 h, 6 h, 12 h, 5 days, 7 days, 10 days, and 14 days injury groups and their preceding groups as shown in Fig. 5b.

Table 2 The average ratios of CB2R to GAPDH in each group (n=5)

Group	Mean±SEM (range)
Control	1.28±0.07 (1.19–1.33)[a]
3 h	1.75±0.13 (1.57–1.90)[b]
6 h	2.11±0.15 (1.94–2.31)[b]
12 h	2.33±0.14 (2.14–2.54)[b]
1 day	2.42±0.11 (2.30–2.59)
3 days	2.29±0.12 (2.17–2.47)
5 days	2.70±0.08 (2.62–2.81)[b]
7 days	2.69±0.07 (2.60–2.76)
10 days	2.28±0.11 (2.11–2.38)[b]
14 days	1.78±0.17 (1.54–1.92)[b]

[a] $p<0.01$ (vs each posttraumatic interval)

[b] $p<0.05$ (vs preceding posttraumatic interval)

Discussion

To forensic pathologists, wound age estimation is a critical issue in routine forensic autopsies which provides indispensable information for the reconstruction of crime scenes and judges the relationship between wounds and cause of death [17–20]. Most researches on forensic wound age determination have been focused on human and murine skin wound healing process in which a variety of biological substances are involved [21–26]. However, forensic wound

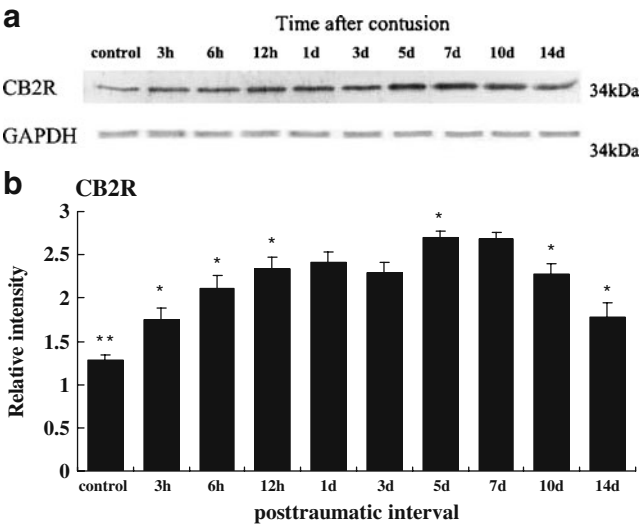

Fig. 4 **a** Analysis of CB2R and GAPDH protein from skeletal muscle specimens by Western blotting. Lane C indicates the result of the control skeletal muscle. Representative results from five individual animals are shown. **b** Relative intensity of CB2R to GAPDH. All values are expressed as the means±SEM (n=5). **$p<0.01$ (vs each posttraumatic group); *$p<0.05$ (vs preceding posttraumatic group)

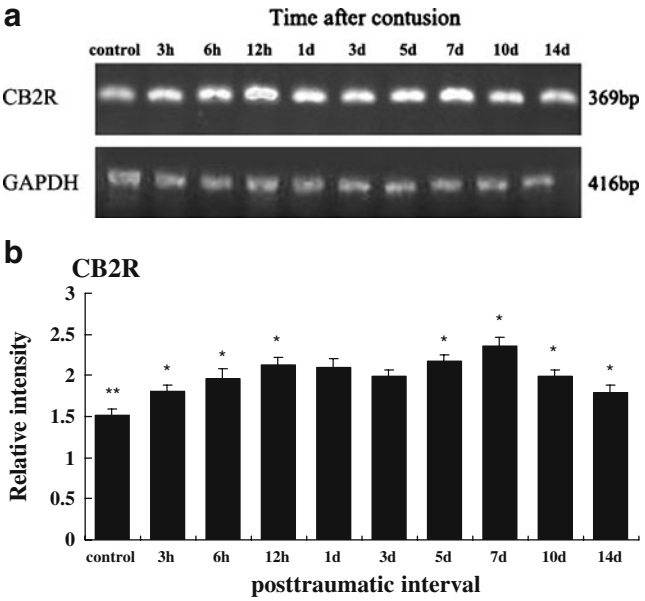

Fig. 5 **a** Analysis of CB2R and GAPDH mRNA expressions from skeletal muscle specimens by RT-PCR. Lane C indicates the result of the control skeletal muscle. Representative results from five individual animals are shown. **b** Relative intensity of CB2R to GAPDH. All values represent the means±SEM (n=5). **$p<0.01$ (vs each posttraumatic group); *$p<0.05$ (vs preceding posttraumatic group)

age estimation for mammalian skeletal muscle has not been given enough attention yet.

To the best of our knowledge, it was the first report describing immunofluorescent localization of CB2R in macrophages of skeletal muscle contusion zones. It is generally acknowledged that muscle damage induces massive macrophages infiltration into injured zones [27, 28], and by 24 h, macrophages are the predominant cell type [29]. In vitro, studies have shown that factors produced by injured skeletal muscle such as fibroblast growth factor and platelet-derived growth factor are highly chemoattractant for both neutrophils and macrophages, and this activity is apparent within muscle tissue 3 h post injury and is enhanced by 24 h [30]. Recent studies confirmed that myogenic precursor cells are also chemotactic for macrophages [31, 32]. There is interesting evidence that CB2R can accommodate the chemotactic response of human macrophages to chemokines CCL2-3 [33], and peritoneal macrophage response to the chemokine RANTES/CCL5 is significantly inhibited by CB2R ligands THC and CP55,940 and by the CB2R-specific agonist O-2137. Meanwhile, the inhibition by THC is reversed by the CB2 receptor-specific antagonist SR144528. THC treatment has a minimal effect on the chemotactic response of $CB2R^{-/-}$ peritoneal macrophages [34]. These findings implicate that CB2R has an effect on the modulation of macrophages in response to chemoattractants. Therefore, we speculate that CB2R is involved in the inflammatory response of macrophages during skeletal muscle contusion.

According to previous study, the expression of troponin I mRNA could give significant information about the age determination of skeletal muscle contusion and rat samples with known post-infliction intervals were employed [35]. There are many studies on the ultrastructure and pathophysiological development of skeletal muscle contusion healing using a mechanical blunt trauma model in rodents [36–38], and it is considered that the experimental model mimicked the damage–repair process in human skeletal muscle with a high degree of accuracy and objectivity. Thus, the results obtained from this model are seemingly applicable to the age determination of skeletal muscle contusion in forensic practices.

Considering the viewpoint of forensic pathological application, the present study demonstrated that the average ratios of CB2R to GAPDH were presumed to be useful for skeletal muscle wound age determination. In Western blotting results, all samples in 5 and 7 days post-injury groups showed ratios of >2.60. After 7 or within 5 days, no samples showed ratios of >2.60. Thus, ratios markedly exceeding 2.60 may strongly indicate a wound age at 5–7 days. It was interesting to note that there was significant difference in the CB2R to GAPDH ratios between 3 and 6 h post-injury as detected by Western blotting and RT-PCR in our study. However, in the previous investigation, immunohistochemical staining was restricted in practical application, especially for the estimation of wound age less than 8 h, because it was not accurate and stable in semi-quantitative analysis, and the results may be influenced by investigators [35]. Thus, in the present study, detection of protein and mRNA by Western blotting and RT-PCR was more suitable for wound age estimation, which was usually more stable and sensitive than immunohistochemical assays. Moreover, up-regulation of cytokine or enzyme mRNA is usually earlier than the one of their protein, it was more appropriate to detect mRNA by RT-PCR in early wound age estimation [39]. The more exact expression tendency for wound age estimation might be described by Western blotting and RT-PCR. Based on our results, if Western blotting and RT-PCR were used in combination with morphological analysis, the ranges of wound age estimation would be narrowed further.

In conclusion, we investigated dynamic distribution and expression of CB2R, indicating that CB2R might be involved in modulating macrophages in response to inflammatory event in rat skeletal muscle wound healing. CB2R is available as a marker for wound age determination, which would provide a new perspective on wound age estimation.

Acknowledgment This study was financially supported in part by grants from research funds for the Doctoral Program funded by Ministry of Education of China (200801590020) and National Natural Science Foundation of China (30271347).

References

1. Munro S, Thomas KL, Abu-Shaar M (1993) Molecular characterization of a peripheral receptor for cannabinoids. Nature 365:61–65
2. Kishimoto S, Muramatsu M, Gokoh M, Oka S, Waku K, Sugiura T (2005) Endogenous cannabinoid receptor ligand induces the migration of human natural killer cells. J Biochem 137:217–223
3. Oka S, Ikeda S, Kishimoto S, Gokoh M, Yanagimoto S, Waku K, Sugiura T (2004) 2-arachidonoylglycerol, an endogenous cannabinoid receptor ligand, induces the migration of EoL-1 human eosinophilic leukemia cells and human peripheral blood eosinophils. J Leukoc Biol 76:1002–1009
4. Facci L, Dal Toso R, Romanello S, Buriani A, Skaper SD, Leon A (1995) Mast cells express a peripheral cannabinoid receptor with differential sensitivity to anandamide and palmitoylethanolamide. Proc Natl Acad Sci U S A 92:3376–3380
5. Matias I, Pochard P, Orlando P, Salzet M, Pestel J, Di Marzo V (2002) Presence and regulation of the endocannabinoid system in human dendritic cells. Eur J Biochem 269:3771–3778
6. Galiègue S, Mary S, Marchand J, Dussossoy D, Carrière D, Carayon P, Bouaboula M, Shire D, Le Fur G, Casellas P (1995) Expression of central and peripheral cannabinoid receptors in human immune tissues and leukocyte subpopulations. Eur J Biochem 232:54–61

7. Mackie K (2006) Cannabinoid receptors as therapeutic targets. Annu Rev Pharmacol Toxicol 46:101–122
8. Buckley NE (2008) The peripheral cannabinoid receptor knockout mice: an update. Br J Pharmacol 153:309–318
9. Brown AJ (2007) Novel cannabinoid receptors. Br J Pharmacol 152:567–575
10. Wright K, Rooney N, Feeney M, Tate J, Robertson D, Welham M, Ward S (2005) Differential expression of cannabinoid receptors in the human colon: cannabinoids promote epithelial wound healing. Gastroenterology 129:437–453
11. Montecucco F, Lenglet S, Braunersreuther V, Burger F, Pelli G, Bertolotto M, Mach F, Steffens S (2009) CB(2) cannabinoid receptor activation is cardioprotective in a mouse model of ischemia/reperfusion. J Mol Cell Cardiol 46:612–620
12. Bátkai S, Osei-Hyiaman D, Pan H, El-Assal O, Rajesh M, Mukhopadhyay P, Hong F, Harvey-White J, Jafri A, Haskó G, Huffman JW, Gao B, Kunos G, Pacher P (2007) Cannabinoid-2 receptor mediates protection against hepatic ischemia/reperfusion injury. FASEB J 21:1788–1800
13. Ashton JC, Rahman RM, Nair SM, Sutherland BA, Glass M, Appleton I (2007) Cerebral hypoxia–ischemia and middle cerebral artery occlusion induce expression of the cannabinoid CB2 receptor in the brain. Neurosci Lett 412:114–117
14. Muñoz-Luque J, Ros J, Fernández-Varo G, Tugues S, Morales-Ruiz M, Alvarez CE, Friedman SL, Arroyo V, Jiménez W (2008) Regression of fibrosis after chronic stimulation of cannabinoid CB2 receptor in cirrhotic rats. J Pharmacol Exp Ther 324:475–483
15. Cavuoto P, McAinch AJ, Hatzinikolas G, Janovská A, Game P, Wittert GA (2007) The expression of receptors for endocannabinoids in human and rodent skeletal muscle. Biochem Biophys Res Commun 364:105–110
16. Lighthall JW (1988) Controlled cortical impact: a new experimental brain injury model. J Neurotrauma 5:1–15
17. Takamiya M, Saigusa K, Kumagai R, Nakayashiki N, Aoki Y (2005) Studies on mRNA expression of tissue-type plasminogen activator in bruises for wound age estimation. Int J Legal Med 119:16–21
18. Kondo T (2007) Timing of skin wounds. Leg Med 9:109–114
19. Takamiya M, Fujita S, Saigusa K, Aoki Y (2008) Simultaneous detection of eight cytokines in human dermal wounds with a multiplex bead-based immunoassay for wound age estimation. Int J Legal Med 122:143–148
20. Ishida Y, Kimura A, Takayasu T, Eisenmenger W, Kondo T (2008) Expression of oxygen-regulated protein 150 (ORP150) in skin wound healing and its application for wound age determination. Int J Legal Med 122:409–414
21. Guan DW, Ohshima T, Kondo T (2000) Immunohistochemical study on Fas and Fas ligand in skin wound healing. Histochem J 32:85–91
22. Kondo T, Ohshima T, Mori R, Guan DW, Ohshima K, Eisenmenger W (2002) Immunohistochemical detection of chemokines in human skin wounds and its application to wound age determination. Int J Legal Med 116:87–91
23. Takamiya M, Saigusa K, Nakayashiki N, Aoki Y (2003) Studies on mRNA expression of basic fibroblast growth factor in wound healing for wound age determination. Int J Legal Med 117:46–50
24. Hayashi T, Ishida Y, Kimura A, Takayasu T, Eisenmenger W, Kondo T (2004) Forensic application of VEGF expression to skin wound age determination. Int J Legal Med 118:320–325
25. Kagawa S, Matsuo A, Yagi Y, Ikematsu K, Tsuda R, Nakasono I (2009) The time-course analysis of gene expression during wound healing in mouse skin. Leg Med 11:70–75
26. Zhao R, Guan DW, Zhang W, Du Y, Xiong CY, Zhu BL, Zhang JJ (2009) Increased expressions and activations of apoptosis-related factors in cell signaling during incised skin wound healing in mice: a preliminary study for forensic wound age estimation. Leg Med 11:S155–S160
27. McLennan IS (1996) Degenerating and regenerating skeletal muscles contain several subpopulations of macrophages with distinct spatial and temporal distributions. J Anat 188:17–28
28. Pimorady-Esfahani A, Grounds MD, McMenamin PG (1997) Macrophages and dendritic cells in normal and regenerating murine skeletal muscle. Muscle Nerve 20:158–166
29. Papadimitriou JM, Robertson TA, Mitchell CA, Grounds MD (1990) The process of new plasmalemma formation in focally injured skeletal muscle fibres. J Struct Biol 103:124–134
30. Robertson TA, Maley MA, Grounds MD, Papadimitriou JM (1993) The role of macrophages in skeletal muscle regeneration with particular reference to chemotaxis. Exp Cell Res 207:321–331
31. Chazaud B, Brigitte M, Yacoub-Youssef H, Arnold L, Gherardi R, Sonnet C, Lafuste P, Chretien F (2009) Dual and beneficial roles of macrophages during skeletal muscle regeneration. Exerc Sport Sci Rev 37:18–22
32. Chazaud B, Sonnet C, Lafuste P, Bassez G, Rimaniol AC, Poron F, Authier FJ, Dreyfus PA, Gherardi RK (2003) Satellite cells attract monocytes and use macrophages as a support to escape apoptosis and enhance muscle growth. J Cell Biol 163:1133–1143
33. Montecucco F, Burger F, Mach F, Steffens S (2008) CB2 cannabinoid receptor agonist JWH-015 modulates human monocyte migration through defined intracellular signaling pathways. Am J Physiol Heart Circ Physiol 294:H1145–H1155
34. Raborn ES, Marciano-Cabral F, Buckley NE, Martin BR, Cabral GA (2008) The cannabinoid delta-9-tetrahydrocannabinol mediates inhibition of macrophage chemotaxis to RANTES/CCL5: linkage to the CB2 receptor. J Neuroimmune Pharmacol 3:117–129
35. Sun JH, Wang YY, Zhang L, Gao CR, Zhang LZ, Guo Z (2010) Time-dependent expression of skeletal muscle troponin I mRNA in the contused skeletal muscle of rats: a possible marker for wound age estimation. Int J Legal Med 124:27–33
36. Hurme T, Kalimo H, Lehto M, Järvinen M (1991) Healing of skeletal muscle injury: an ultrastructural and immunohistochemical study. Med Sci Sports Exerc 23:801–810
37. Huard J, Li Y, Fu FH (2002) Muscle injuries and repair: current trends in research. J Bone Joint Surg Am 84:822–832
38. Wright-Carpenter T, Opolon P, Appell HJ, Meijer H, Wehling P, Mir LM (2004) Treatment of muscle injuries by local administration of autologous conditioned serum: animal experiments using a muscle contusion model. Int J Sports Med 25:582–587
39. Bai R, Wan L, Shi M (2008) The time-dependent expressions of IL-1beta, COX-2, MCP-1 mRNA in skin wounds of rabbits. Forensic Sci Int 175:193–197